available at www.sciencedirect.com

ScienceDirect

journal homepage: www.elsevier.com/locate/carbon

Restoring electrical conductivity of dielectrophoretically assembled graphite oxide sheets by thermal and chemical reduction techniques

Hosung Kang[a], *Atul Kulkarni*[b], *Sasha Stankovich*[c], *Rodney S. Ruoff*[d,*], *Seunghyun Baik*[a,b,e,*]

[a]*SKKU Advanced Institute of Nanotechnology (SAINT), Sungkyunkwan University, Suwon, Gyeonggi-do 440-746, Republic of Korea*
[b]*School of Mechanical Engineering, Sungkyunkwan University, Suwon, Gyeonggi-do 440-746, Republic of Korea*
[c]*Milliken Research Corporation, 920 Milliken Road, Spartanburg, SC 29304, USA*
[d]*Department of Mechanical Engineering, College of Engineering, University of Texas, 1 University Station C2200, Austin, TX 78712-0292, USA*
[e]*Department of Energy Science, Sungkyunkwan University, Suwon, Gyeonggi-do 440-746, Republic of Korea*

ARTICLE INFO

Article history:
Received 24 September 2008
Accepted 31 January 2009
Available online 13 February 2009

ABSTRACT

Thin layers of graphite oxide sheets were dispersed in dimethylformamide and dielectrophoretically assembled onto predefined and opposing metal electrodes. The dielectrophoretic method resulted in the deposition of multiple layers of graphite oxide. After drying, the deposits were then reduced by thermal or chemical methods. Raman spectroscopy and electrical transport measurements revealed that the thermal reduction technique was more effective in restoring electrical conductivity than the chemical reduction method.

1. Introduction

Recent success in depositing monolayer graphite (graphene) has attracted interests due to both the fundamental physics and possibility of constructing devices [1–6]. Graphene has interesting properties because of its 2D geometry [7,8]. A number of methods have been used to deposit graphene from graphite [9,10]. Deposition of single or multiple layers from highly ordered pyrolytic graphite (HOPG) was demonstrated by a micro-mechanical cleavage method [11]. Micro-mechanical cleavage is an effective method for depositing high quality graphene sheets. However, the material deposited is not uniform and controlled deposition on particular locations has not been achieved. The low yield of this approach combined with lack of control of the position of individual sheets limits controlled implementation of highly integrated graphene-based circuits. An important challenge is to obtain individual graphene sheets that are also deposited at desired locations. Rapid thermal expansion of sulfuric acid-intercalated graphite followed by suitable treatment to produce nanoplatelets from the expanded material was also recently demonstrated but these have not been deposited with positional control [12,13].

Graphite oxide is a structured compound obtained by oxidation of graphite [14]. It is typically produced by oxidative treatment of graphite by the “Brodie”, “Hummers”, or “Staudenmaier” methods [15]. The layers in graphite oxide are extensively oxidized and it is yellowish-orange in color compared to graphite. Graphite oxide is an electrically insulating material [16,17]. However, it can be reduced to have less oxygen by thermal or chemical methods that restore the electrical conductivity [18].

There is an interest in integrated circuits at a smaller scale [19] and graphene has been suggested as a conductive sheet upon which nanometer scale devices may be patterned since it can exhibit room temperature ballistic transport over mean

* *Corresponding authors*: Address: SKKU Advanced Institute of Nanotechnology (SAINT), Sungkyunkwan University, Suwon, Gyeonggi-do 440-746, Republic of Korea. Fax: +82 31 290 5889.
E-mail addresses: r.ruoff@mail.utexas.edu (R.S. Ruoff), sbaik@me.skku.ac.kr (S. Baik).
0008-6223/$ - see front matter
doi:10.1016/j.carbon.2009.01.049

free paths up to 300 nm [20]. Dielectrophoresis (DEP) can be an effective tool for manipulating nanoparticles suspended in liquids [21,22]. We recently demonstrated the deposition of thick layers of thermally expanded graphite oxide soot (GO-soot) particles by dielectrophoresis [22]. GO-soot was prepared by rapid thermal expansion of graphite oxide, and the thickness of the deposited layer was greater than 1 μm. In this study, thin layers of graphite oxide were dispersed in dimethylformamide (DMF) and assembled across opposing electrode by DEP. Then the electrical conductivity of the deposited and dried graphite oxide sheets was restored by chemical or thermal treatments. The deposited and treated samples were characterized using Raman spectroscopy, Scanning Electron Microscopy (SEM), Atomic Force Microscopy (AFM), and electrical transport measurements.

2. Experimental

Graphite oxide was synthesized from SP-1 graphite powder (Bay City Carbon) by a modified Hummers method [23]. It was readily exfoliated by sonication in DMF (Aldrich, anhydrous, 99.8%). The graphite oxide was dispersed in DMF at a mass ratio of 9.6×10^{-3} (wt%). The mixture was sonicated at 135 W for 10 min (5510R-DTH, BRANSONIC).

Microelectrodes were fabricated using a conventional photolithographic method. As shown in Fig. 1a, one chip contains seven pairs of Au electrodes with a gap of 2 μm. A 5 nm thick titanium layer and a 200 nm thick gold layer were vapor-deposited (EVACO-41SC, DR Vacuum) on the SiO_2-on-Si substrate as a top electrode material. Graphite oxide sheets dispersed in DMF were deposited across the opposing electrodes using DEP. A drop of the mixture (0.5 μl) was placed onto electrodes on the gap, and an alternating current electric field (10 V_{pp}, 100 kHz; 33220A, Agilent) was applied for 1 min. The droplet was then blown off using nitrogen gas (99.8% purity). The reproducibility of dielectrophoretic deposition was good. The graphite oxide sheets were successfully deposited onto 136 opposing microelectrodes from 140 attempts.

The electrical conductivity of the deposited graphite oxide sheets was restored using chemical or thermal treatments. Hydrazine hydrate, mixed with deionized water at a volume ratio of 1:100, was used for the chemical treatment procedure; the substrate with the deposited graphite oxide sheets was immersed in such a solution held at 100 °C. The exposure to hydrazine in water was continued until there was no change in the conductivity of the deposit on the chip although oxide groups were not perfectly removed. For the thermal reduction, the cylindrical quarts tube was initially vacuumized using a rotary pump. Then it was pressurized to 800 mm Hg using argon gas (>99.999% purity). Finally, values were closed and the argon atmosphere was stationary during the experiments. The as-deposited graphene oxide sheets were heat-treated at 200 or 400 °C. The heating rate was 1 °C/min. The samples were kept at the constant temperature for a designated time and then naturally cooled down to room temperature for measurements using SEM (JEOL JSM-7401F), Raman spectroscopy (Kaiser optical system model RXN1), AFM (Veeco diINNOVA 840-012-711) and a semiconductor parameter analyzer (Agilent E5262A). A rapid thermal reduction technique was also tested. In this case, the quartz tube was pre-heated while argon gas was continuously supplied at 60 ml/min. The thermocouple indicated that the temperature of argon gas inside the tube was 1000 °C. The chamber lid was open during the experiments. The sample was inserted into the tube for 20 s and then rapidly removed. The estimated temperature of the sample, calculated using a simple lumped capacitance method and a natural convection coefficient on horizontal plate, was about 1000 °C [24].

3. Results and discussion

Graphite oxide sheets can be dispersed in DMF and this enables use of DEP to assemble them across the microelectrodes. Fig. 1b shows an SEM image of such sheets deposited across the electrodes. A number of different DEP conditions, such as the applied voltage, frequency and time, were tested with the goal of depositing the minimum thickness of graphite oxide sheets. The selected parameters were 10 V_{pp}, 100 kHz and 1 min. An AFM image is shown in the inset of Fig. 1b and a height measurement is provided in Fig. 1c. The thickness of an individual layer of graphene oxide is typically obtained as about 1 nm [25]. It is clear from the AFM data that thin layers of graphite oxide sheets were typically deposited by DEP and the sheets were also folded and overlapped in

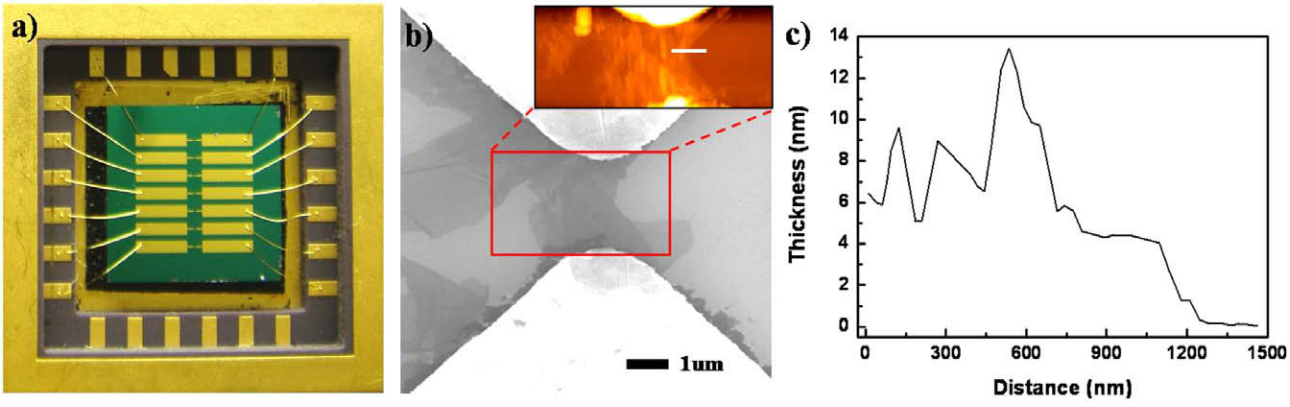

Fig. 1 – Graphite oxide sheets assembled between 2 μm gap electrodes using DEP. (a) One chip contains seven identical electrodes. (b) SEM image, the inset shows an AFM image. (c) AFM section profiles along the line in Fig. 1b.

some regions. The AFM scan shows step heights ranging from 4 to 13 nm. This indicates that 4–13 layers of graphite oxide were deposited considering the typical thickness of graphite oxide of about 1 nm. Another possibility is that the same sheet was folded multiple times. It has been demonstrated that graphite oxide can be reduced by heating [25]. As mentioned, two separate thermal treatments at 200 and 400 °C were used. The resistance change of the graphite oxide sheets was monitored as a function of time is shown in Fig. 2. The heat treatment time during the constant temperature exposure segment is shown on the x-axis; i.e. the ramp time is not included. Before heating, the resistance of the deposited sheet material was found to be infinite, which agrees with the conclusions of others that graphite oxide is essentially an insulating material [16,17]. At 200 °C, the resistance was measured after 60 min and the first value recorded was 553 kΩ. The resistance initially decreased rapidly but then reached a steady state value at longer times. At 400 °C, the resistance increased at longer times after the initial rapid decrease. This could be due to the thermal decomposition of graphite oxide sheets during the prolonged heat treatment time at an elevated temperature; i.e. transformation of graphite oxide into CO and/or CO_2 gas [25,26]. As shown in Fig. 2b, graphite oxide could not be observed between the electrodes after 15 h of heat treatment at 400 °C, and the resistance reached infinity. It is also possible that a small amount of oxygen, perhaps not completely removed from the tube, led to the complete oxidation of all carbon in the deposit.

Fig. 3a shows an SEM image of the graphite oxide sheets after 2 h of exposure at 200 °C (identical deposit as shown in Fig. 1a). The AFM image provided in the inset shows a noticeable change after the thermal reduction. Figs. 1b and 3b show a large decrease in the thickness of the deposit from the heat treatment. It is well known that, in the case of deposition from an aqueous dispersion of graphite oxide, the deposit has overlapped and stacked graphite oxide layers with interlamellar water. Evaporation of a significant fraction of this water by heating yields a significant reduction in thickness. It is reasonably likely that interlamellar DMF is playing the same role here, and also that the as-deposited (by DEP) over-

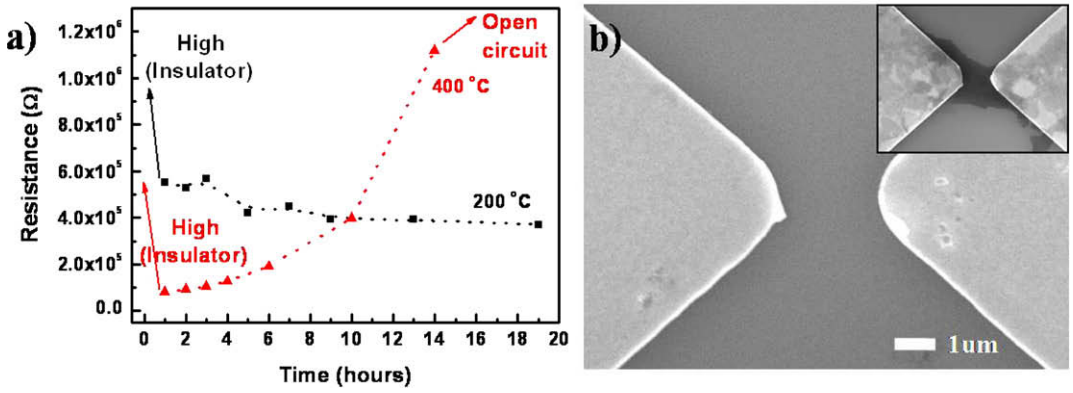

Fig. 2 – The resistance change of the graphite oxide sheets as a function of the heat treatment time. (a) The process was carried out at 200 or 400 °C. (b) SEM image of the graphite oxide deposited electrode after 15 h of heat treatment at 400 °C. The inset image shows graphite oxide sheets deposited on the identical electrode before the heat treatment.

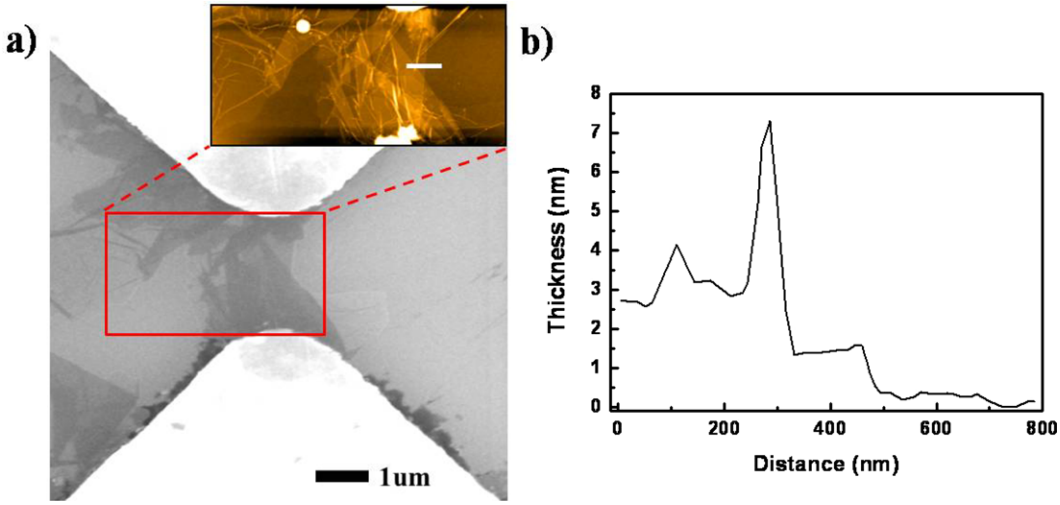

Fig. 3 – Dielectrophoretically assembled graphite oxide sheets after 2 h of thermal reduction at 200 °C. (a) SEM image. The inset shows a magnified AFM image. (b) AFM section profiles along the line in the inset.

lapped layers might conceivably pick up water during exposure to ambient. Another contribution to the reduction in thickness of the deposit might be caused by the changes in chemistry occurring directly in the graphite oxide sheets themselves. The thickness of the reduced graphite oxide ranged from 1.5 to 7.5 nm. This suggested approximately 4–22 layers were deposited assuming that the thickness of a single layer of graphene is 0.34 nm.

We calculated resistivities of thermally reduced deposits on 10 opposing microelectrode pairs assuming rectangular parallelepiped geometries. The length was considered as 2 μm which is the gap of electrode. The average width and thickness was about as 1 μm and 3 nm each. The average resistivity was estimated to be $3.5 \times 10^{-4}\ \Omega\,m$. This is higher than the natural resistivity of graphite ($1.2 \times 10^{-6}\ \Omega\,m$) [27]. The value reported here for these deposits is influenced by the contact resistance, error from the approximation of the geometry of the deposit, and incomplete reduction. The ballistic transport in graphene was destroyed by the incompletely reduced oxide groups demonstrating the limitation of this approach. The oxygen was not completely removed.

A rapid thermal reduction experiment was also carried out [26,28]. The graphite oxide deposited on opposing electrodes was rapidly inserted into a pre-heated quartz tube (at 1000 °C) for 20 s. Argon gas was continuously supplied to the quartz tube at 1 atm pressure. Electrical transport measurements were carried out after the sample was rapidly removed and cooled down to room temperature. Fig. 4 shows the change in source-drain current before and after the rapid thermal treatment and as a function of the source-drain voltage. The final resistance of the deposit was similar to that of the slow heat treatment as shown in Fig. 2. Perhaps such short time exposures to high temperature can be used to thermally reduce dielectrophoretically deposited graphite oxide sheets.

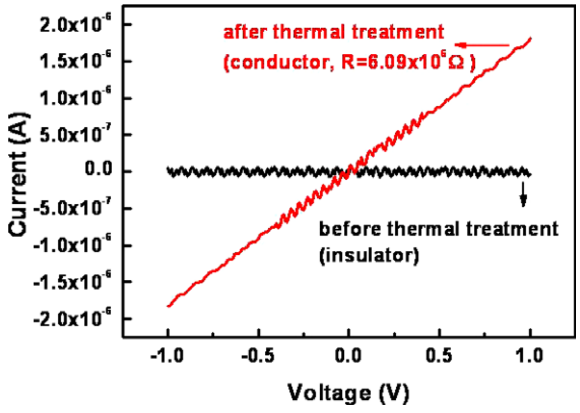

Fig. 4 – Electrical transport measurements before and after the rapid thermal treatment at 1000 °C.

An attempt to chemically reduce the dielectrophoretically deposited graphite oxide sheets was also made. Fig. 5a shows an SEM image before the chemical treatment. As shown in Fig. 5b, the resistance decreased with time and reached a steady state after 40 min of exposure to the aqueous hydrazine solution. Hydrazine is also known to etch silicon; Grigaliunasa et al. reported an etching rate of 2 μm/min using a diluted hydrazine solution [29]. For this reason, exposure to the aqueous hydrazine solution was carried out for 2 days in order to investigate the etching phenomena of both silicon and silicon dioxide. The inset in Fig. 5b shows an SEM image after this chemical treatment demonstrating severe etching of the silicon–silicon dioxide substrate. Hydrazine hydrate acts as a reducing agent and reacts with a variety of materials including oxide layers of substrates. This indicates that the chemical reduction approach with hydrazine could be problematic for device applications of graphite oxide sheets on silicon.

Raman spectroscopy was used in an attempt to assess possible reduction of the dielectrophoretically deposited graphite oxide sheets [30]. Fig. 6 compares Raman spectra taken before and after the chemical and thermal reduction. The Raman spectrum of as-prepared graphite oxide deposits displays two prominent peaks at 1350 and 1598 cm^{-1} that correspond to the D and G modes, respectively [9,30,31]. The G mode is related to the vibration of sp^2-hybridized carbon. The phonon mode at 1330 cm^{-1}, also known as the D mode, corresponds to the conversion of a sp^2-hybridized carbon to a sp^3-hybridized carbon [31,32]. The increase in the intensity of the D band can be interpreted as the destruction of graphite sp^2 structures or covalently attached functional groups. Fig. 6a shows a change in Raman spectra with respect to the chemical treatment time. As shown in Fig. 6, the area under the D mode was

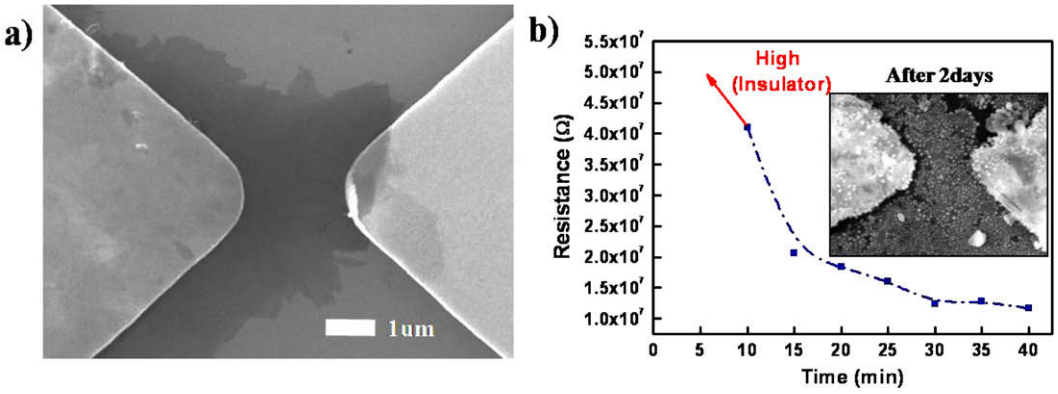

Fig. 5 – Chemical reduction of dielectrophoretically deposited graphite oxide sheets. (a) SEM image before the reduction. (b) Change in resistance as a function of the chemical treatment time. The inset shows an SEM image after 2 days of reduction.

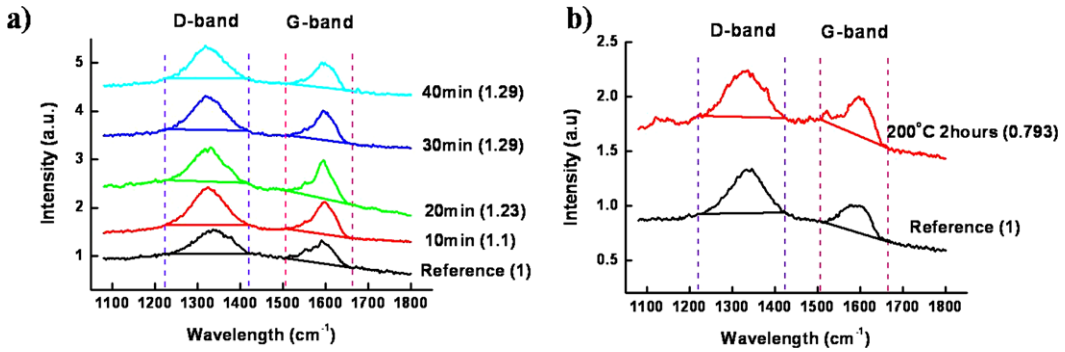

Fig. 6 – Raman spectra taken before and after the reduction. The normalized area ratio of D/G mode is provided in the parenthesis next to the treatment time. (a) Chemical reduction approach, (b) thermal reduction approach.

integrated from 1220 to 1420 cm^{-1}, and that under the G mode was integrated from 1510 to 1660 cm^{-1}. The baseline of the integration is also shown in Fig. 6. The normalized D/G area ratio is shown in the parenthesis. The D/G area ratio was normalized by that of the dielectrophoretically deposited graphite oxide sheets obtained before the chemical treatment. The normalized D/G area ratio, shown in the parentheses, increased with the chemical treatment time, which is consistent with the observation of Stankovich et al. [10], Ferrari et al. [30]. A number of cracks developed at the surface of graphite oxide, which could increase the D/G area ratio as a function of the chemical treatment time despite the reduction of the oxide groups. This could be the reason of the observed phenomenon [10,30]. As shown in Fig. 6b, the normalized D/G ratio decreased after 2 h of thermal reduction at 200 °C due to the removal of oxide groups [33]. This suggests that, at least in terms of the type of chemical treatment used here, the heat treatment approach might be more appropriate for restoring sp^2 carbon regions in the dielectrophoretically deposited graphite oxide sheets.

4. Conclusion

Graphite oxide sheets were dispersed in DMF and DEP was used to selectively deposit such sheets onto opposing microelectrodes. The current approach resulted in the deposition of multiple layers of graphite oxide. The deposits were then partially reduced after drying. Electrical and Raman spectroscopic measurements revealed that the simple heat treatment was more effective in restoring electrical conductivity than by exposure to aqueous hydrazine solution. In this manner, selective deposition of chemically modified and electrically conductive graphite sheets was achieved. Thus, the dielectrophoretic deposition combined with post-reduction has potential for large-scale deposition of graphite oxide sheets for device applications.

Acknowledgments

This research was supported by WCU(World Class University) program through the Korea Science and Engineering Foundation funded by the Ministry of Education, Science and Technology (R31-2008-000-10029-0) and by a Grant from Center for Nanoscale Mechatronics and Manufacturing, one of the 21st Century Frontier Research Programs supported by Ministry of Science and Technology, Korea. RSR appreciates support from the NSF and the DARPA iMINT Center of the USA.

REFERENCES

[1] Novoselov KS, Geim AK, Morozov SV, Jiang D, Katsnelson MI, Grigorieva IV, et al. Two-dimensional gas of massless Dirac fermions in graphene. Nature 2005;438(7065):197–200.
[2] Novoselov KS, Geim AK, Morozov SV, Jiang D, Zhang Y, Dubonos SV, et al. Electric field effect in atomically thin carbon films. Science 2004;306(5296):666–9.
[3] Novoselov KS, McCann E, Morozov SV, Falko VI, Katsnelson MI, Zeitler U, et al. Unconventional quantum Hall effect and Berry's phase of 2 pi in bilayer graphene. Nat Phys 2006;2(3):177–80.
[4] Zhang YB, Tan YW, Stormer HL, Kim P. Experimental observation of the quantum Hall effect and Berry's phase in graphene. Nature 2005;438(7065):201–4.
[5] Heersche HB, Jarillo-Herrero P, Oostinga JB, Vandersypen LMK, Morpurgo AF. Bipolar supercurrent in graphene. Nature 2007;446(7131):56–9.
[6] Roddaro S, Pingue P, Piazza P, Pellegrini V, Beltram F. The optical visibility of graphene: interference colors of ultrathin graphite on SiO_2. Nano Lett 2007;7(9):2707–10.
[7] Wang JJ, Zhu MY, Outlaw RA, Zhao X, Manos DM, Holloway BC, et al. Free-standing subnanometer graphite sheets. Appl Phys Lett 2004;85(7):1265–7.
[8] Stankovich S, Piner RD, Chen XQ, Wu NQ, Nguyen ST, Ruoff RS. Stable aqueous dispersions of graphitic nanoplatelets via the reduction of exfoliated graphite oxide in the presence of poly(sodium 4-styrenesulfonate). J Mater Chem 2006;16(2):155–8.
[9] Stankovich S, Dikin DA, Dommett GHB, Kohlhaas KM, Zimney EJ, Stach EA, et al. Graphene-based composite materials. Nature 2006;442(7100):282–6.
[10] Stankovich S, Dikin DA, Piner RD, Kohlhaas KA, Kleinhammes A, Jia Y, et al. Synthesis of graphene-based nanosheets via chemical reduction of exfoliated graphite oxide. Carbon 2007;45(7):1558–65.
[11] Novoselov KS, Jiang D, Schedin F, Booth TJ, Khotkevich VV, Morozov SV, et al. Two-dimensional atomic crystals. PNAS 2005;102(30):10451–3.
[12] Chen GH, Weng WG, Wu DJ, Wu CL, Lu JR, Wang PP, et al. Preparation and characterization of graphite nanosheets from ultrasonic powdering technique. Carbon 2004;42(4):753–9.

[13] Chen GH, Wu DJ, Weng WU, Wu CL. Exfoliation of graphite flake and its nanocomposites. Carbon 2003;41(3):619–21.
[14] Hirata M, Gotou T, Horiuchi S, Fujiwara M, Ohba M. Thin-film particles of graphite oxide 1: high-yield synthesis and flexibility of the particles. Carbon 2004;42(14):2929–37.
[15] Jeong HK, Lee YP, Lahaye RJWE, Park MH, An KH, Kim IJ, et al. Evidence of graphitic AB stacking order of graphite oxides. J Am Chem Soc 2008;130(4):1362–6.
[16] Bourlinos AB, Gournis D, Petridis D, Szabo T, Szeri A, Dekany I. Graphite oxide: chemical reduction to graphite and surface modification with primary aliphatic amines and amino acids. Langmuir 2003;19(15):6050–5.
[17] Xiao P, Xiao M, Liu PG, Gong KC. Direct synthesis of a polyaniline-intercalated graphite oxide nanocomposite. Carbon 2000;38(4):626–8.
[18] He H, Klinowski J, Forster M, Lerf A. A new structure model of graphite oxide. Chem Phys Lett 1998;287:53–6.
[19] Gilje S, Han S, Wang M, Wang KL, Kaner RB. A chemical route to graphene for device applications. Nano Lett 2007;7(11):3394–8.
[20] Meyer JC, Geim AK, Katsnelson MI, Novoselov KS, Booth TJ, Roth S. The structure of suspended graphene sheets. Nature 2007;446(7131):60–3.
[21] Krupke R, Hennrich F, Lohneysen H, Kappes MM. Separation of metallic from semiconducting single-walled carbon nanotubes. Science 2003;301(5631):344–7.
[22] Hong S, Jung S, Kang SJ, Kim YJ, Chen X, Stankovich S, et al. Dielectrophoretic deposition of graphite oxide soot particles. J Nanosci Nanotechnol 2008;8:1–4.
[23] Cai D, Song M. Preparation of fully exfoliated graphite oxide nanoplatelets in organic solvents. J Mater Chem 2007;17:3678–80.
[24] Incropera FP, Dewitt DP, Bergman TL, Lavine AS. Fundamentals of heat and mass transfer. 6th ed. John Wiley and Sons, Inc.; 2006.
[25] Hung CC, Corbin J. Synthesis and thermal stability of graphite oxide-like materials. Carbon 1997;37:701–5.
[26] McAllister MJ, Li JL, Adamson DH, Schniepp HC, Abdala AA, Liu J, et al. Single sheet functionalized graphene by oxidation and thermal expansion of graphite. Chem Mater 2007;19(18):4396–404.
[27] Powell RL, Childs GE. American Institute of Physics Handbook. 1972. p. 4–160.
[28] Schniepp HC, Li JL, McAllister MJ, Sai H, Herrera-Alonso M, Adamson DH, et al. Functionalized single graphene sheets derived from splitting graphite oxide. J Phys Chem B 2006;110(17):8535–9.
[29] Grigaliunasa V, Tamulevicius S, Niaura G, Kopustinskas G, Gudonyte A, Jucius D. Imprint lithography of pyramidal photonic pillars using hydrazine etching. Physica E 2003;16:568–73.
[30] Ferrari AC, Meyer JC, Scardaci V, Casiraghi C, Lazzeri M, Mauri F, et al. Raman spectrum of graphene and graphene layers. Phys Rev Lett 2006;97(18):187401-1–4.
[31] Dresselhaus MS, Dresselhaus G, Jorio A, Souza Filho AG, Saito R. Raman spectroscopy on isolated single wall carbon nanotubes. Carbon 2002;40(12):2043–61.
[32] Bronikowski MJ, Willis PA, Colbert DT, Smith KA, Smalley RE. Gas-phase production of carbon single-walled nanotubes from carbon monoxide via the HiPco process: a parametric study. J Vac Sci Technol A 2001;19(4):1800–5.
[33] Kudin KN, Ozbas B, Schniepp HC, Prudhomme RK, Aksay IA, Car R. Raman spectra of graphite oxide and functionalized graphene sheets. Nano Lett 2008;8(1):36–41.